New Journal of Physics
The open-access journal for physics

# Density profile and polymer configurations for a polymer melt in a regular array of nanotubes

**Tiago P Peixoto and Barbara Drossel**
Institut für Festkörperphysik, TU Darmstadt, Hochschulstraße 6,
64289 Darmstadt, Germany
E-mail: tiago@fkp.tu-darmstadt.de and barbara@fkp.tu-darmstadt.de

*New Journal of Physics* **13** (2011) 073030 (16pp)
Received 24 January 2011
Published 22 July 2011
Online at http://www.njp.org/
doi:10.1088/1367-2630/13/7/073030

**Abstract.** By using two generic polymer models, namely self-consistent field theory and bond-fluctuation Monte-Carlo simulations, we investigate numerically the properties of a polymer melt in a hexagonal array of nanotubes as a function of the polymer length, the interaction with the nanotubes and the compressibility or average density. The combined effect of the attractive interaction with the nanotube walls, the entropy decrease due to the impenetrability of the walls and the hexagonal arrangement of the nanotubes with varying gap size in between them leads to a wide array of possible density profiles and polymer configurations as a function of the model parameters. Even in the case of the Monte-Carlo simulations, where the contact interaction affects only the first layer of monomers, the effect of the wall can nevertheless be felt throughout the entire melt at intermediate temperatures.

## Contents

**1. Introduction** **2**
**2. Self-consistent field theory** **3**
2.1. Model . . . 3
2.2. Density profiles . . . 5
2.3. Polymer conformation . . . 5
**3. Monte Carlo: bond fluctuation** **8**
3.1. Model . . . 8
3.2. Density profiles . . . 10
3.3. Radius of gyration . . . 11
**4. Discussion** **13**
**Acknowledgments** **15**
**References** **15**

## 1. Introduction

The investigation of polymer–nanotube mixtures is of great technological importance. Composites made of polymer and carbon nanotubes have excellent mechanical, thermal and electrical properties [1–9]. A major challenge in producing high-quality nanocomposites lies in achieving a good dispersal of the nanotubes and preventing them from sticking together during the formation of the material. One pathway taken to achieve this goal is to synthesize a hexagonal array of carbon nanotubes on a template and then let a polymer melt infiltrate the space between the nanotubes [10]. This process is facilitated by the attractive interaction between polymers and nanotubes. When the polymer can be made to fill the space between the tubes, the goal of producing a composite material in which the nanotubes are well dispersed has been achieved.

However, materials that consist of a hexagonal array of nanotubes with polymers in the spaces between the tubes are not only technologically important, but also interesting from a theoretical point of view. Owing to the presence of the nanotubes, the configurations of the polymers are no longer random walks as in a bulk melt, but they wind around the tubes and squeeze in the gaps between the tubes. If the distance between the tubes is not too long, the configurations of all polymers will be affected strongly by the presence of the tubes. Furthermore, due to the decreased entropy in the vicinity of the tubes, the polymer density decreases close to the tubes.

The goal of this paper is to study the density profile and the polymer conformations of a polymer melt in a regular hexagonal nanotube array. Since we are interested in the general features of polymers confined in the space between a hexagonal array of cylinders, we use simple idealized models for polymers and nanotubes, which are modeled as Gaussian chains or as walks on a lattice. By comparing the results obtained by two different methods, we can identify the generic properties of such systems. The first method is self-consistent field theory (SCFT) [11–13] for a polymer melt between cylindrical impenetrable tubes, which model the nanotubes, with an attractive interaction between tubes and polymers. The second method is Monte-Carlo simulations with a bond-fluctuation model, which incorporates the same type of interaction with the nanotubes. We evaluate two equilibrium features: the density profile of

the polymer melt and the radius of gyration of the polymers as a function of their position. This study considerably extends our preliminary first analysis presented in [10], where the two methods have been introduced and where the relaxation time towards equilibrium and a few density profiles and polymer configurations have been evaluated in the absence of an attractive interaction.

Here, we calculate the rich variety of density profiles and polymer configurations that can be obtained by varying three important model parameters, namely the strength of the attractive interaction with the nanotube walls, the average polymer density or compressibility and the temperature. Our Monte-Carlo simulations show that the presence of the nanotubes affects the polymer melt throughout the entire volume, even though only the first monomer layer interacts with the tubes. This effect vanishes at lower temperatures, when a layer of monomer becomes adsorbed at the surface of the tubes, isolating them from the bulk.

This paper is structured as follows. In section 2, we describe the analysis based on the SCFT and show the results for the polymer density and configurations obtained numerically. In section 3, we present a complementary approach using bond-fluctuation Monte-Carlo simulations and show the results of computer simulations. Finally, in section 4 we compare and discuss the results obtained by the two approaches.

## 2. Self-consistent field theory

### 2.1. Model

In accordance with the SCFT approach [11–13], we consider a system of $n$ polymers in a volume $V$, where the individual chains are treated as perfect Gaussian chains with degree of polymerization $l$ and statistical segment length $a = 1$, with an associated end-to-end distance $R_e = a\sqrt{l}$. We assume that the melt is compressible [14], leading to a factor dependent on the polymer concentration profile $\phi(\boldsymbol{r})$ in the partition function

$$Z = \frac{1}{n!}\int \prod_{\alpha} D[\boldsymbol{r}_\alpha]P[\boldsymbol{r}_\alpha]\exp\left\{-\frac{\rho\kappa l}{2}\int_V \mathrm{d}^3 r[(\hat{\phi}-\phi_0)^2 + u\hat{\phi}]\right\}, \tag{1}$$

where $\alpha$ labels the individual chains, $l$ is the degree of polymerization, $\rho$ is the volume per monomer, $\kappa$ is a dimensionless constant proportional to the inverse isothermal compressibility, $\phi_0$ is the average concentration in the melt and $P[\boldsymbol{r}_\alpha]$ is the weight factor for a Gaussian chain configuration,

$$P[\boldsymbol{r}(s)] \sim \exp\left[-\frac{3}{2R_e^2}\int_0^1 \mathrm{d}s\left(\frac{\mathrm{d}\boldsymbol{r}}{\mathrm{d}s}\right)^2\right]. \tag{2}$$

We further consider that the system is in equilibrium with an external reservoir of bulk material with average concentration $\bar{\phi}_B = \phi_0$, with which it can freely exchange polymers. The field $u(\boldsymbol{r})$ is an attractive interaction potential with the nanotube array and is defined as

$$u(\boldsymbol{r}) = -\frac{\gamma\exp[-\lambda(|\boldsymbol{r}-\boldsymbol{r}_c|-R_t)]}{k_B T}, \tag{3}$$

where $\boldsymbol{r}_c$ is the center of the closest nanotube, $R_t$ is the nanotube radius, and $\gamma$ and $\lambda$ define the interaction strength and range, respectively (we fixed the range to $\lambda = 1$ and varied the interaction strength $\gamma$). The partition function can be rewritten so that the relevant term

corresponds to the partition function of a single chain subjected to an external field $w$ which incorporates the effect of the remaining chains and of the nanotubes,

$$Q[w] = \frac{1}{V}\int D[\boldsymbol{r}]P[\boldsymbol{r}]\exp\left\{-\frac{1}{V}\int_V \mathrm{d}^3 r\left(\mathrm{i}w + \frac{\rho\kappa l}{2}u\right)\phi^{\mathrm{sc}}\right\}. \tag{4}$$

The end-segment distribution $q(\boldsymbol{r}, s)$ of a single chain can be obtained from the following diffusion equation,

$$\frac{\partial q(\boldsymbol{r}, s)}{\partial s} = \frac{R_{\mathrm{e}}^2}{6}\nabla^2 q(\boldsymbol{r}, s) - \left(\mathrm{i}w(\boldsymbol{r}) + \frac{\rho\kappa l}{2}u(\boldsymbol{r})\right)q(\boldsymbol{r}, s), \tag{5}$$

with $q(\boldsymbol{r}, 0) = 1$, where the impenetrability of the nanotubes is implemented by the boundary condition $q(\boldsymbol{r}_{\mathrm{t}}, s) = 0$ (corresponding to $w(\boldsymbol{r}_{\mathrm{t}}) = \infty$), where $\boldsymbol{r}_t$ denotes the surface of the nanotubes. The concentration profile imposed by a given field is obtained from

$$\phi(r) = \frac{\bar{\phi}}{Q}\int_0^1 \mathrm{d}s q(\boldsymbol{r}, s)q(\boldsymbol{r}, 1-s), \quad Q = \frac{1}{V}\int \mathrm{d}^3 r q(\boldsymbol{r}, 1). \tag{6}$$

The average concentration $\bar{\phi}$ can be obtained from the equilibrium condition with the bulk, by requiring that the chemical potential in the system and in the reservoir be equal. From equation (1), we obtain

$$\mu = k_{\mathrm{B}}T[\ln\rho\bar{\phi} - \ln Q]. \tag{7}$$

The chemical potential in the bulk is thus given by $\mu_{\mathrm{B}} = k_{\mathrm{B}}T[\ln\rho\bar{\phi}_{\mathrm{B}} + (\bar{\phi}_{\mathrm{B}} - \phi_0)\frac{\rho\kappa l}{2})]$, where $\bar{\phi}_{\mathrm{B}}$ is the concentration in the bulk. By setting $\mu = \mu_{\mathrm{B}}$, we obtain

$$\bar{\phi} = \bar{\phi}_{\mathrm{B}}Q\exp\left\{(\bar{\phi}_{\mathrm{B}} - \phi_0)\frac{\rho\kappa l}{2}\right\}, \tag{8}$$

which can be substituted in equation (6). The field generated by the concentration profile is obtained by minimizing the free energy, which leads to

$$\frac{w}{\rho\kappa l} + \mathrm{i}(\phi - \phi_0)^2 = 0. \tag{9}$$

The self-consistency of equation (9) can be satisfied by solving this equation for $\phi$, using equations (5) and (6), based on the method described in [15, 16].

The nanotubes are aligned in the $z$-direction. Due to the translational invariance, we performed our calculations on a two-dimensional (2D) unit cell of a hexagonal lattice with periodic boundary conditions. In the following, we used arbitrary length units and their corresponding volume units. The polymer number density $\rho$ is set to one inverse volume unit, and the radius of the nanotubes is set to 20 length units. The total size of the unit cell is 100 units in the $x$-direction and $100/\sqrt{3} \approx 58$ units in the $y$-direction, which leads to a spacing of $50(1 + 1/\sqrt{3})^{1/2} - 40 \approx 22.8$ units between the nanotubes. This configuration is inspired by the values used in the experiments [10], and by the expectation that the confinement effects are more interesting when the nanotube spacing is of the order of the nanotube radius. The volume occupation of the polymer melt in the bulk reservoir was set to $\bar{\phi}_{\mathrm{B}} = \phi_0 = 0.95$. We used several values of the degree of polymerization $l$ (and hence $R_{\mathrm{e}}$) and of the inverse isothermal compressibility $\kappa$. While higher values of $\kappa$ are more relevant for the experiments, we also used smaller values in order to explore the entire range of possibilities. In order to differentiate between the effects of confinement and of the impenetrable barrier imposed by nanotubes, we considered also a system composed of free polymers confined only by a single impenetrable flat wall, with the same attractive potential as in equation (6), and with $\phi_0 = 0.95$ in the bulk.

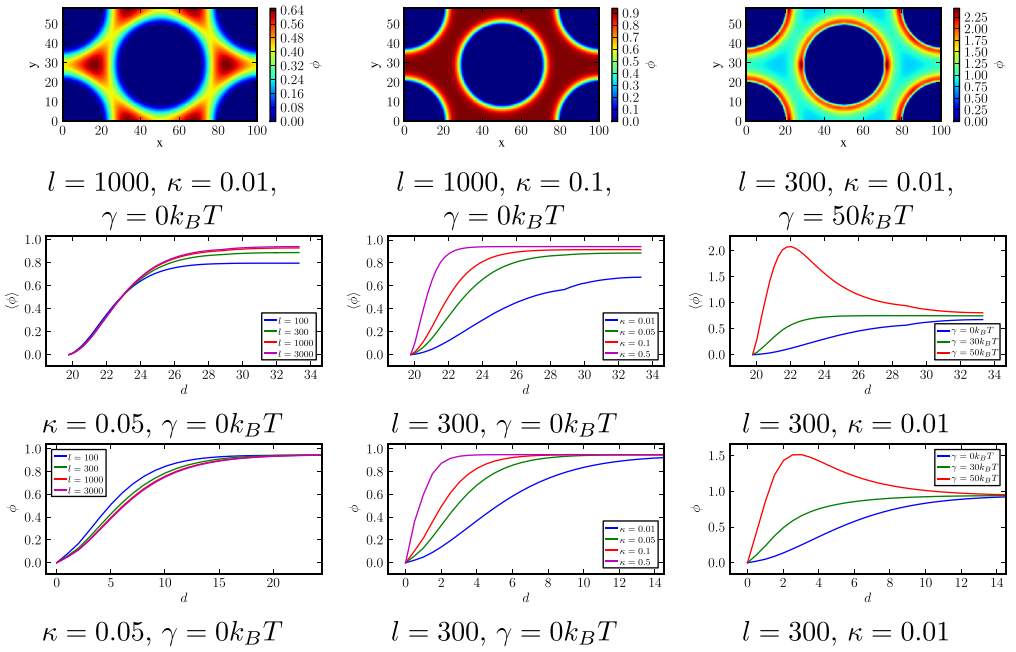


**Figure 1.** Concentration profiles obtained by SCFT for different combinations of $\gamma$, $l$ and $\kappa$. Top row: 2D profiles. Middle row: 1D average profiles as a function of the center of the closest nanotube. Bottom row: 1D profiles for polymers confined by a single impenetrable attractive wall.

### 2.2. *Density profiles*

The polymer density profiles obtained with the above approach are shown in figure 1. The top row shows three examples for the full density distribution, the middle row shows average density as a function of the distance from the center of the closest nanotube and the bottom row for the system composed of a single wall. The concentration in the melt increases with increasing $\kappa$ and $\gamma$. A larger $\kappa$ implies a smaller compressibility, making deviations from the equilibrium density $\phi_0$ more difficult. A larger $\gamma$ implies a stronger attraction between the nanotube walls and the polymers, favoring larger densities close to the walls. With increasing degree of polymerization $l$, the density profile becomes independent of $l$ for $\gamma = 0$, as expected with our choice of scaling. The depletion zone close to the nanotubes is due to the fact that the nanotube wall cannot be penetrated by the polymer. Further away from the nanotubes, the density comes close to the bulk equilibrium value $\phi_0$. If the distance between the nanotubes was made larger, all density profiles would eventually reach this asymptotic value. In this situation, the concentration profile is essentially the same as that for a single impenetrable flat wall. The bulk density is reached faster when $\kappa$ is larger.

### 2.3. *Polymer conformation*

The polymer conformations were investigated by modeling individual chains as biased random walks, which are independently affected by the effective potential $w$ imposed by the melt. This was done by performing several 3D walks of length $l$ where each step $i$ of equal size 1 is chosen randomly in all directions with probability proportional to the end-segment distribution

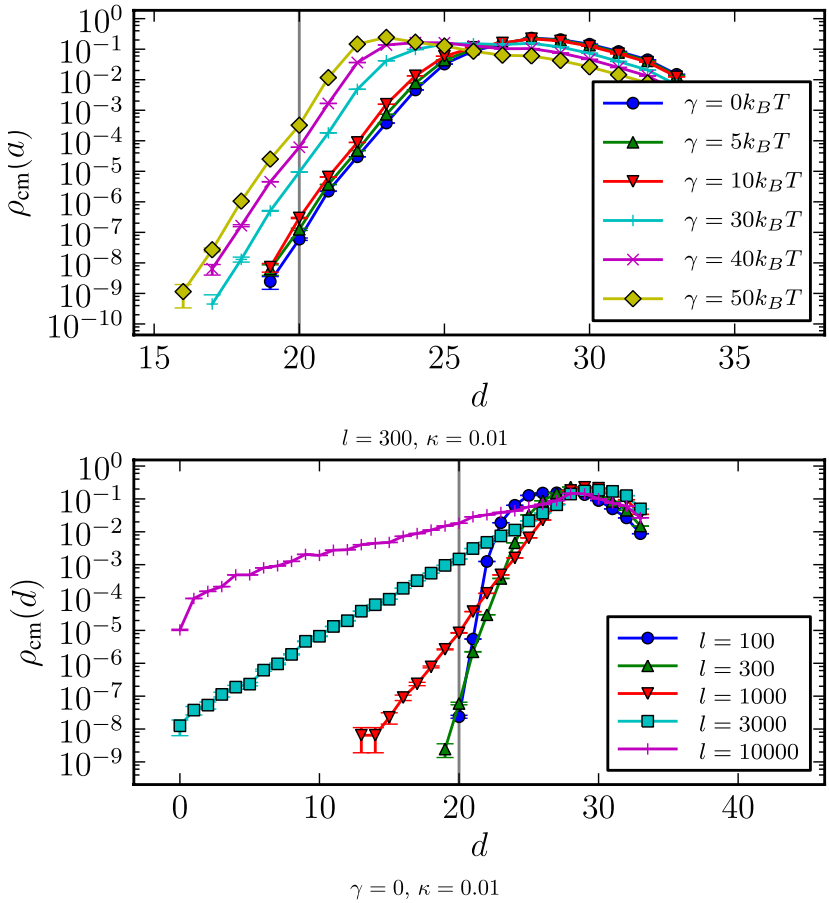


**Figure 2.** Distribution of the center of mass as a function of the distance from the center of the closest nanotube for different values of $\gamma$ and $l$, as obtained within the SCFT.

$q(\boldsymbol{r}, i/l) \times q(\boldsymbol{r}, 1-i/l)$, obtained previously. The quantities measured were the center of mass of the chains, and the contributions to the squared radius of gyration $R_g^2$ of the $z$- and $xy$-directions, as well as the total radius of gyration. Figure 2 shows the distribution of the center of mass as a function of the distance from the center of the closest nanotube. When we increase the interaction strength $\gamma$, the peak of the distribution moves closer to the nanotubes, as expected. The distribution decreases close to the nanotube walls, because the polymers cannot penetrate the wall. However, the center of mass of a polymer can be inside the nanotube (i.e. at a distance smaller than 20 from the nanotube center), because polymers are able to wrap around the nanotubes. This effect is stronger in the case of longer polymers. The decrease of the distribution with increasing distance is due to the fact that fewer points have such long distances from the closest nanotube.

Figure 3 illustrates the influence of the attractive interaction with the walls on the average squared radius of gyration $R_g^2$ as a function of the distance of the center of mass of the polymer from the center of the closest nanotube. Figure 4 shows the effect of polymer length on the radius of gyration. In the $z$-direction, the polymers are not influenced by the nanotubes, due to the translational invariance of the system, and the $z$-part of $R_g^2$ is constant. In the $xy$-direction, the radius of gyration increases close to the walls, which must be due to the fact that the

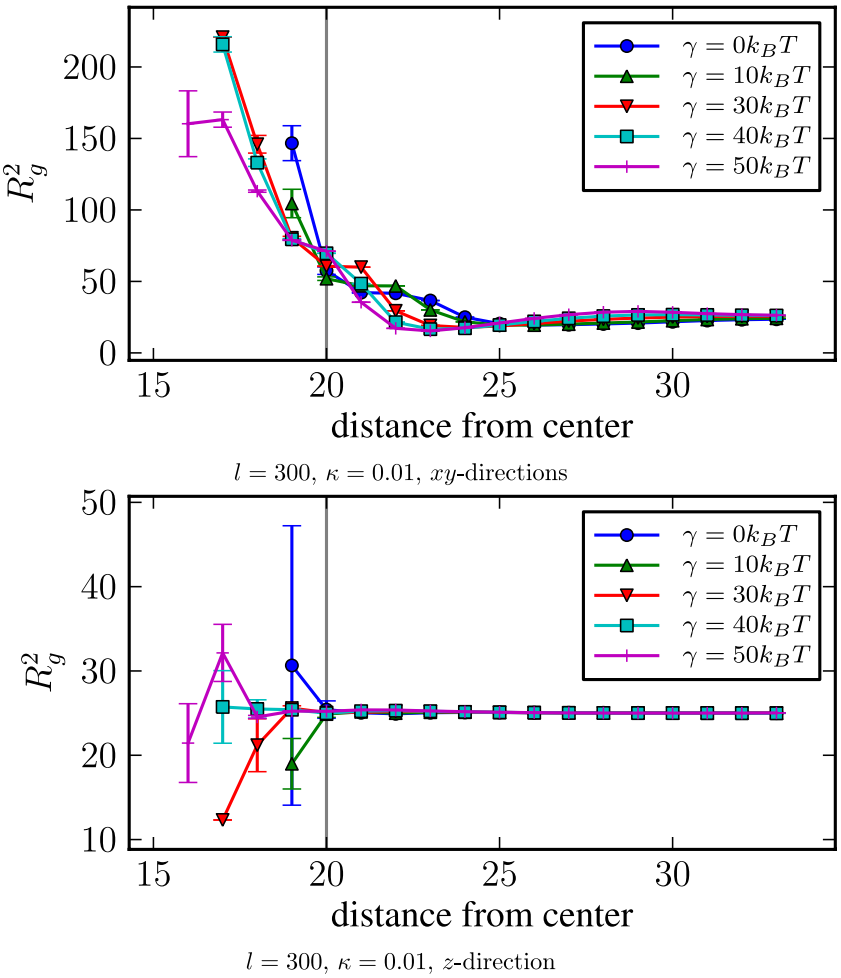


**Figure 3.** Average radius of gyration as a function of the distance from the center of the closest nanotube with and without an attractive interaction with the wall, as obtained with the SCFT. The top and bottom graphs show the contribution of the $xy$-directions and of the $z$-direction to $R_g^2$, respectively.

polymers wrap around the nanotubes. This effect becomes stronger in the presence of attractive interaction. For shorter polymers, the curves have a local minimum, due to these polymers being squeezed into the narrow part of the gap between the nanotubes. Longer polymers can extend into the wider parts of the gap and therefore the minimum is not visible in the data for $R_g^2$ at larger $l$. When we increase the polymer length, polymers that have their center of mass at the longest possible distance from the walls become more squeezed together, since they must fit into the space between the three neighboring nanotubes. This explains the decrease of $R_g^2/l$ with increasing $l$ at larger $d$. Finally, when we increase $l$, the curves for $R_g^2/l$ at $l > 1000$ become flatter, since these very long polymers extend over several nanotubes, and the distance to the closest nanotube contains less information.

Figure 5 shows examples of the full 2D distribution of the center of mass and of the radius of gyration for a very long polymer.

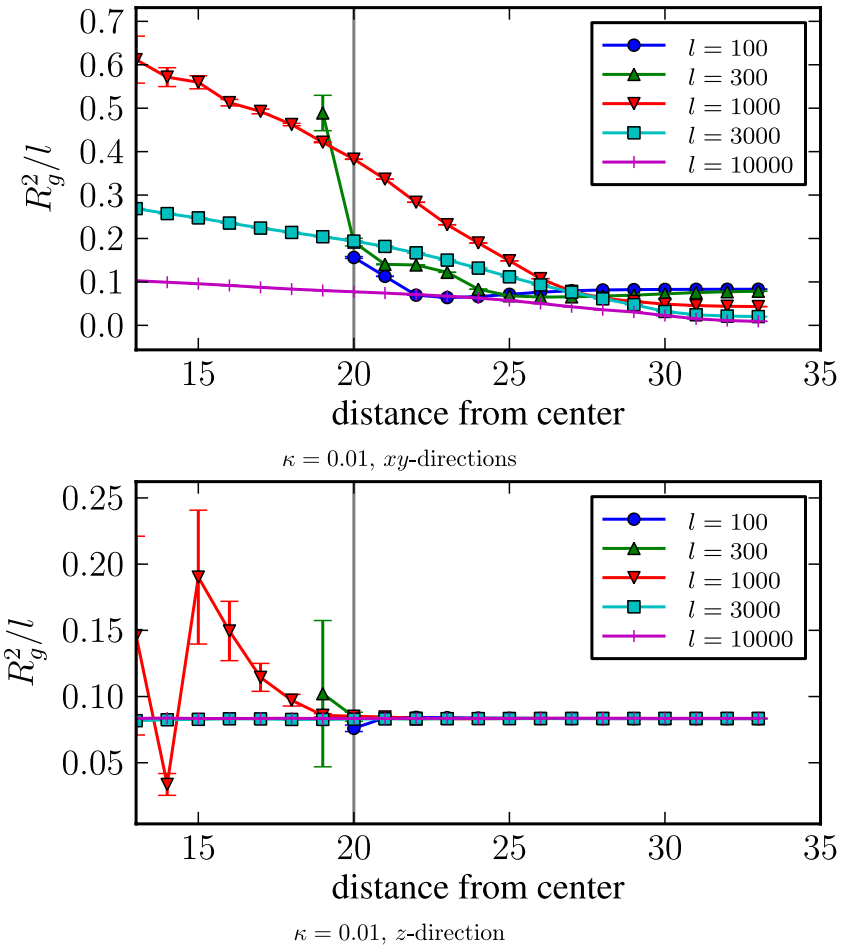


**Figure 4.** Average radius of gyration as a function of the distance from the closest nanotube for different values of $l$ and for $\gamma = 0$, as obtained with SCFT.

## 3. Monte Carlo: bond fluctuation

### *3.1. Model*

We performed Monte-Carlo simulations using one of the variants of the bond fluctuation model [17–23]. Here, we use the simplest version introduced by Shaffer [22]: polymers of length $l$ were placed on a cubic lattice such that each of the individual monomer units occupies a different lattice position and the bond between them occupies a different position in the associated bond lattice, which permits diagonal bonds of length 1, $\sqrt{2}$ and $\sqrt{3}$. In this way, both excluded volume and non-crossing of the chains are guaranteed. We note that this approach allows us to reach monomer concentrations close to 1, comparable to the SCFT case for high $\kappa$, which is the situation that prevails in experiments. Just as we did in the case of the SCFT, we considered one unit cell of the hexagonal array with periodic boundary conditions, with the lattice dimensions being $N_x = 100$, $N_y = 58$ and $N_z = 100$. As in the SCFT configuration, the radius of each nanotube was set to 20 lattice sites, which leads to a spacing between the

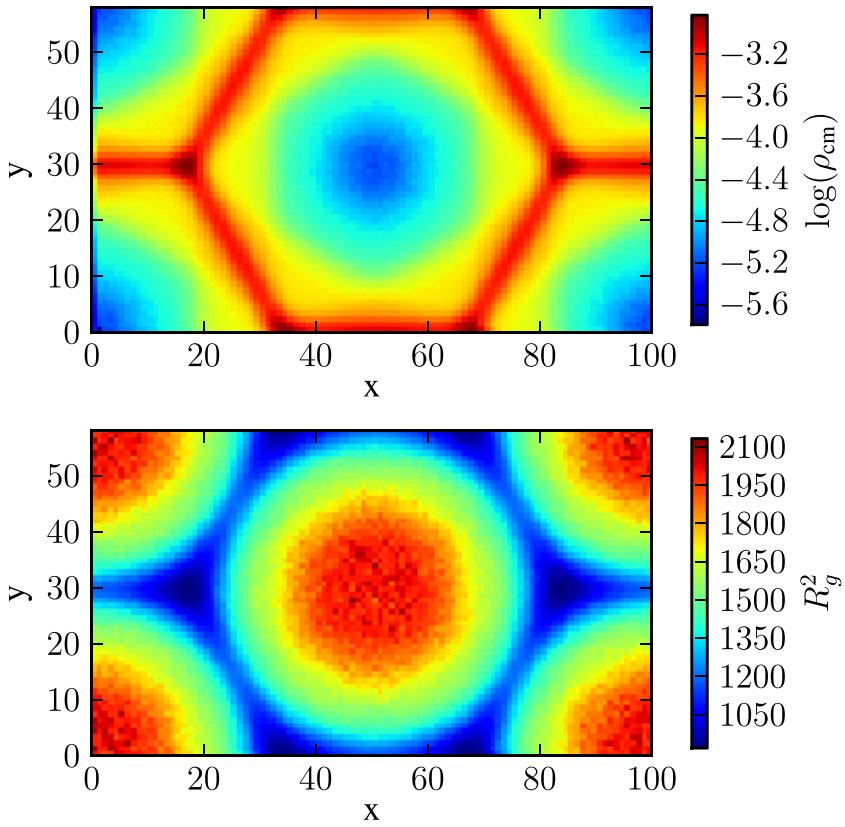


**Figure 5.** 2D distribution of the center of mass (top) and $R_g^2$ (bottom) for $l = 10\,000$, $\kappa = 0.01$ and $\gamma = 0 k_B T$, as obtained with SCFT.

nanotubes of at least 22 sites (which is enough to avoid ergodicity barriers, since it is larger than the average radius of gyration of the chains considered). We also included an interaction between the monomers and the nanotubes, by considering an energy contribution of $-1 k_B T$ for each monomer directly touching the nanotube, and the temperature $T$ was varied. Thus, in contrast to SCFT, the interaction is only due to direct contact with the nanotubes. However, the range of the interaction (1 length unit) is comparable in the two models.

The simulations were initialized with the individual chains regularly stretched along the $z$-direction. The system was equilibrated by using the Metropolis–Hastings algorithm [24, 25]: at each step, a single monomer move was attempted and accepted if it was valid and if the energy difference $\Delta E$ was negative or zero. If the energy difference was positive, it was accepted with a probability proportional to $\exp(-\Delta E / T)$. Additionally, at each time step a reptation move was attempted, where the monomer of a random end of a chain was moved to the other end, and was accepted or not according to the same criterion. The system was evolved at infinite temperature until the average radius of gyration had reached equilibrium. Then the system was evolved at the desired temperature until conformational equilibrium was reached again. Equilibration was verified by observing that the average radius of gyration in all three directions had reached a stationary value.

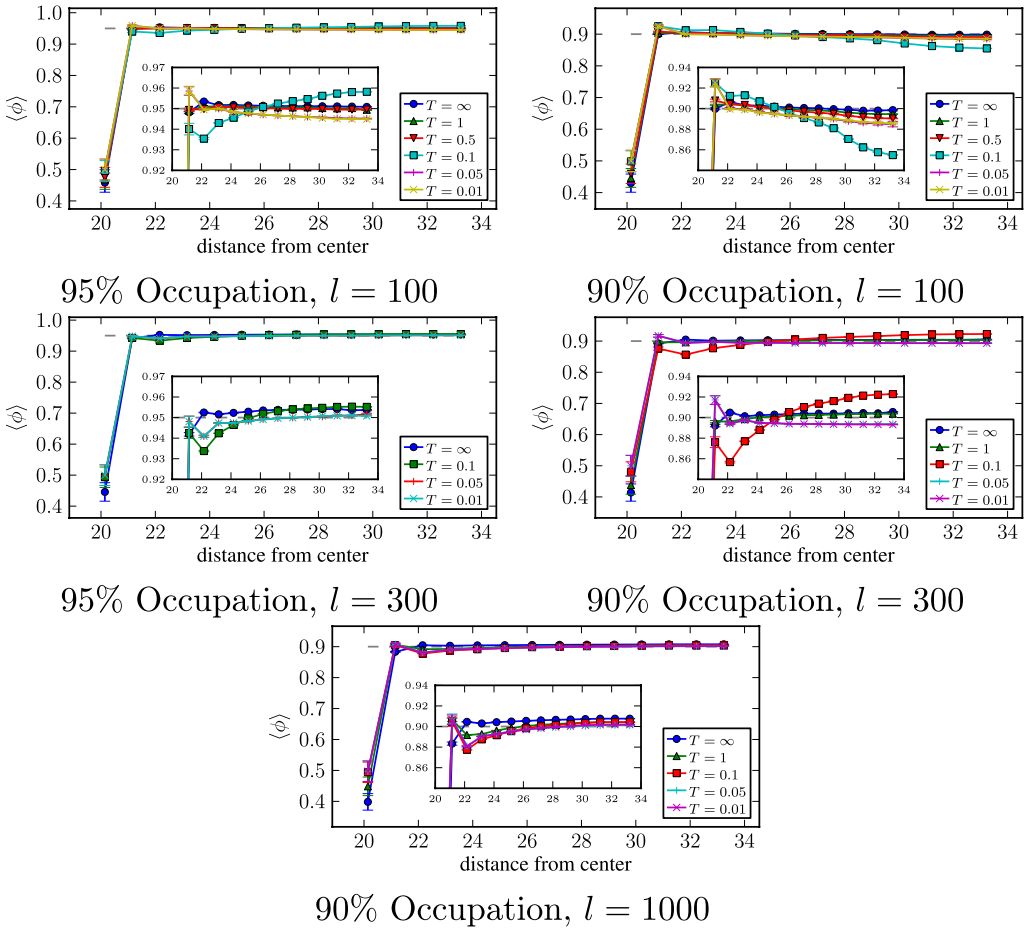


**Figure 6.** Density profile obtained with the bond-fluctuation model for different polymer lengths $l$ and different lattice occupations.

### *3.2. Density profiles*

Figures 6 and 7 show the density profiles obtained for varying $l$, $T$ and total density. The density is defined here as the fraction of occupied lattice sites. For infinite temperature, a depletion zone can be observed, similarly to SCFT. The profiles show only small density variations with $d$. For the lower temperature values, there is a local maximum at $d = 21$, which corresponds to a distance of one lattice site to the nanotube wall. For higher temperature values, the entropic effects dominate close to the wall, and the curves have a local minimum at $d = 21$. For intermediate temperatures, most curves show both effects, i.e. a local maximum at $d = 21$ and a minimum at $d = 22$, because the attractive interaction at $d = 21$ and the entropic effects close to the wall are both important. The monomers touching the nanotubes shield the walls from the other monomers, which then perceive a noninteracting impenetrable wall at $d = 21$. The depletion zone is most pronounced for intermediate temperatures, leading to a positive slope of the density profile over a large distance. An exceptional case is the case $l = 100$ with $o = 90\%$, where the minimum has vanished. The lower density, combined with the shorter length, apparently causes a larger fraction of polymers close to the wall to have contact with the wall, resulting in an energy gain that is always larger than the entropy loss.

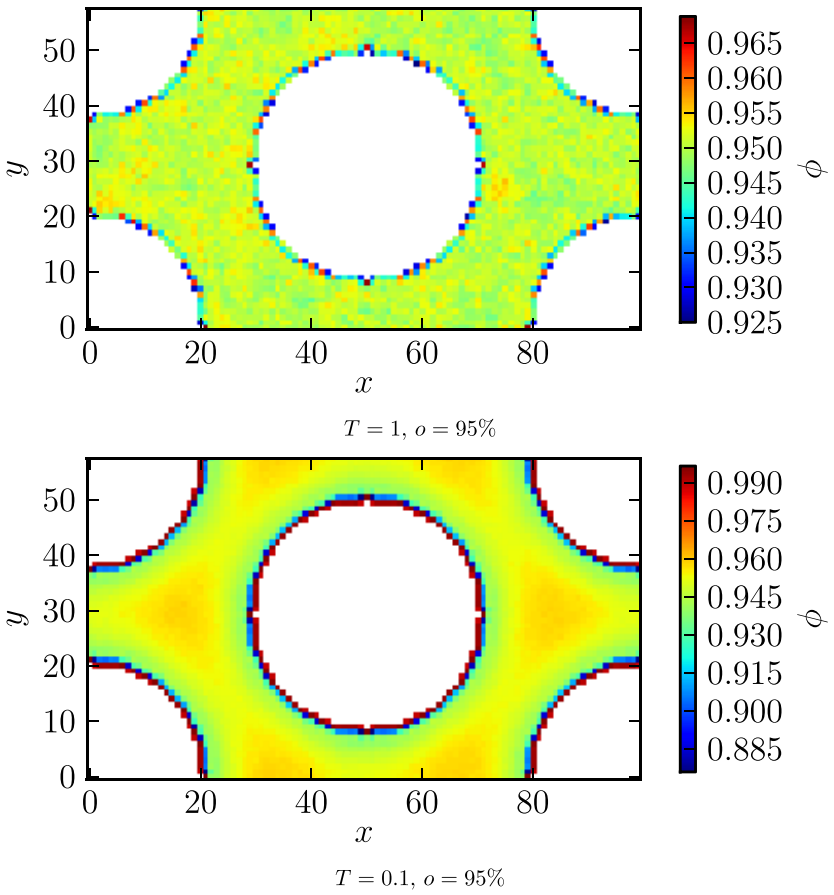


**Figure 7.** 2D density profile obtained with the bond-fluctuation model for $l = 100$, $o = 95\%$ and different temperatures.

### *3.3. Radius of gyration*

Figures 8 and 9 show the $xy$ and the $z$ contributions to the squared radius of gyration of the polymers plotted against the distance $d$ of the center of mass of the polymers from the center of the closest nanotube for two different concentrations. Similarly to the SCFT results, the radius of gyration in the $xy$-plane increases when the center of mass approaches the center of the nanotubes, which is simply a geometrical necessity. In contrast to the SCFT simulations, there is now a slight variation in the $z$-component, which is more clearly visible for lower temperatures, shorter polymers or lower lattice occupations. The reason is that polymers that are close to the nanotubes can stick to the tubes with part of their monomers, which stretches them also in the $z$-direction and makes them more extended in the $z$-direction than they are in the bulk. For somewhat higher temperatures, this stretching effect is manifest further into the bulk, due to higher mobility of the polymers between the wall and the bulk. When polymers are shorter and when density is higher, polymers that are centered in the vicinity of the nanotubes are squeezed into a smaller volume than polymers in the bulk and have smaller values of $R_g^2$, as can be concluded from the shallow minimum visible in the curves for the $xy$ contribution. For

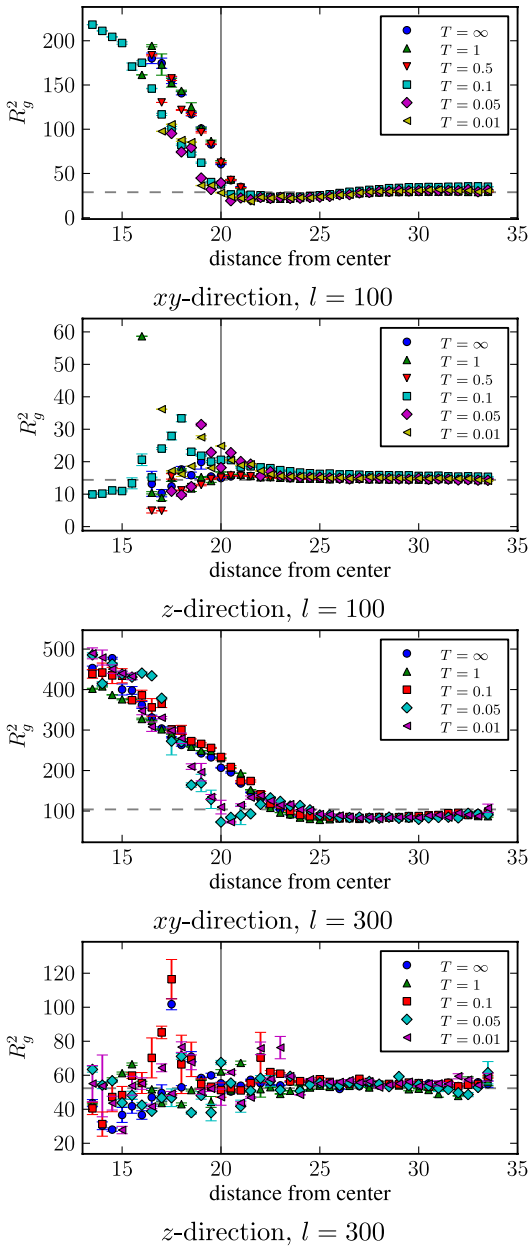


**Figure 8.** Average squared radius of gyration as a function of the distance to the closest nanotubes, obtained with the bond-fluctuation model, for an occupation of 95%. The dashed lines correspond to the average values in the bulk when no nanotubes are present.

larger polymers ($l = 300$), the values of $R_g^2$ in the vicinity of the tubes decrease for smaller temperatures. This is due to the almost complete adsorption of individual chains at the surface of nanotubes, which causes them to be more segregated from each other and thus more coiled (see figure 10).

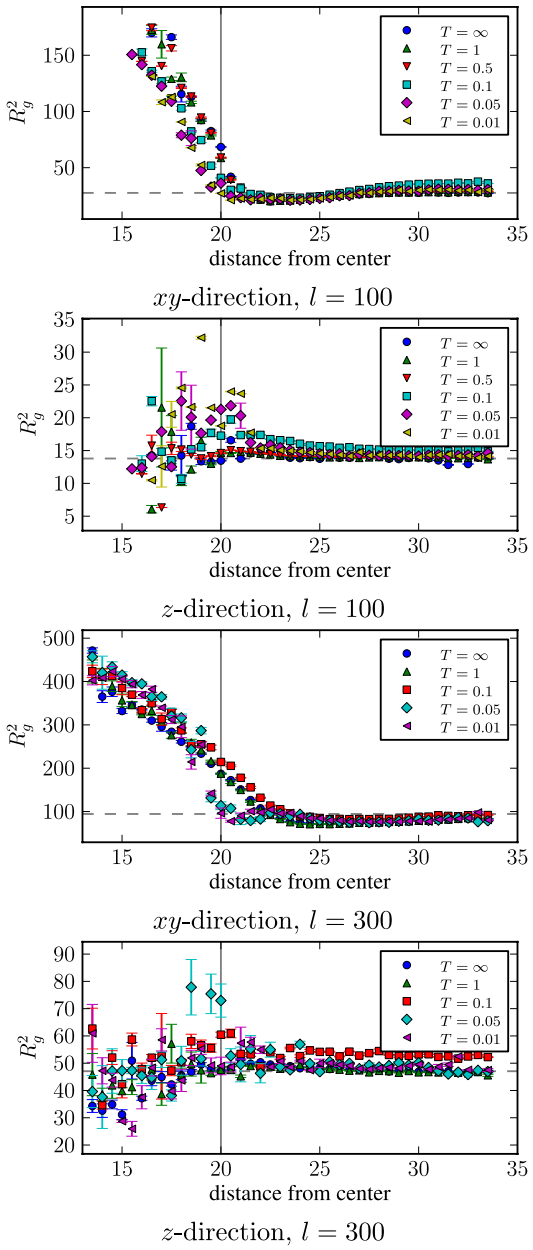


**Figure 9.** Average squared radius of gyration as a function of the distance to the closest nanotubes, obtained with the bond-fluctuation model, for an occupation of 90%. The dashed lines correspond to the average values in the bulk when no nanotubes are present.

## 4. Discussion

We have analyzed the general properties of a polymer melt confined in a regular array of carbon nanotubes, which were modeled as attractive, impenetrable barriers. Using SCFT we obtained the density profile of the melt, depending on the isothermal compressibility, chain length and interaction strength with the nanotubes. The concentration profile shows a higher concentration

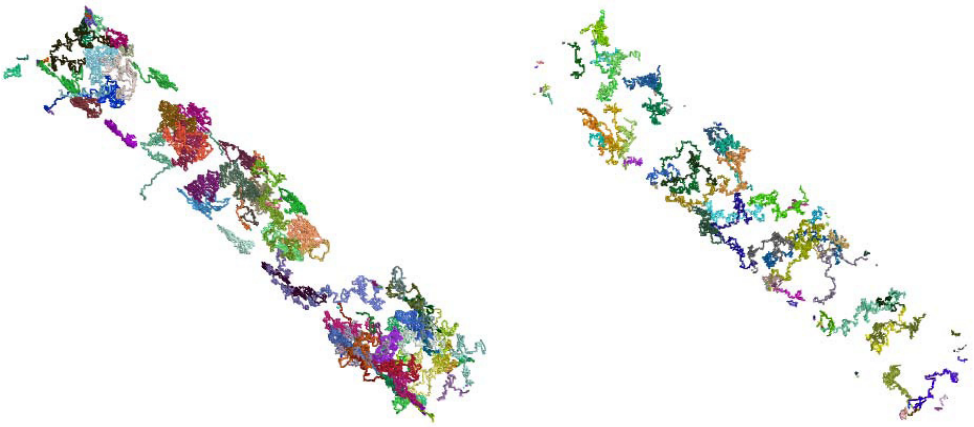


**Figure 10.** Randomly sampled chains with $l = 300$ and center of mass close to the selected nanotube for 95% occupation and two different values of the temperature.

in the larger interstices between the tubes, for larger polymer chains. The interaction with the nanotubes has the expected effect of increasing the concentration in their vicinity. We also obtained polymer conformations within the framework of SCFT by numerically investigating individual chains that interact with the self-consistent effective potential, by means of biased random walks. In this mean-field description, the polymer conformation is affected solely by the density profile and by the geometrical constraints imposed by the confinement.

As an alternative approach, we performed Monte-Carlo simulations with the bond fluctuation model. Since each chain is considered individually, this method provides more detailed information about their conformation at the expense of neglecting other aspects such as compressibility. Additionally, the interaction with the nanotubes was specified more realistically, and the continuously varying potential was replaced by a contact interaction. Analogously to SCFT, we also investigated the density and conformation profiles.

The choice $\lambda = 1$ for the SCFT simulations means that the range of the attractive interaction with the wall is comparable in both types of investigations. However, due to the difference between a contact energy and an exponentially decaying interaction and between an ideal Gaussian chain and a self-avoiding walk on a lattice, the results of the two investigations differ in several aspects. In particular, the small compressibility in the bond fluctuation model results in much more uniform densities and much narrower depletion zones. However, the nature of the interaction potential and the more detailed conformational information provided by this approach allowed us to identify more precisely the effect of the nanotube interaction on the chains close to it, which can become adsorbed at the surface if the temperature is low enough. More interestingly, for intermediate values of temperature, the effects of interaction (both in the chain conformation and in the monomer density) are felt also in the bulk, and the whole melt is affected by the confinement.

We point out that the quality of the Monte-Carlo simulations with the bond-fluctuation model is not affected by the excluded volume of the nanotubes, which is not large enough to cause ergodicity problems. In such situations, it is expected that both the bond-fluctuation and off-lattice models display similar behavior [26].

## Acknowledgments

We thank Marcus Müller and Kostas Ch Daoulas for useful discussions. We also acknowledge the priority program SPP 1369 of the DFG for funding this work under contract number Dr300/5 and for providing the computer cluster in which all the simulations and computations were carried out.

## References

[1] Sandler J, Shaffer M S P, Prasse T, Bauhofer W, Schulte K and Windle A H 1999 Development of a dispersion process for carbon nanotubes in an epoxy matrix and the resulting electrical properties *Polymer* **40** 5969

[2] Barrau S, Demont P, Peigney A, Laurent C and Lacabanne C 2003 DC and AC conductivity of carbon nanotubes–polyepoxy composites *Macromolecules* **36** 5187–94

[3] Kim Y J, Shin T S, Choi H D, Kwon J H, Chung Y-C and Yoon H G 2005 Electrical conductivity of chemically modified multiwalled carbon nanotube/epoxy composites *Carbon* **43** 23–30

[4] Ahmad K, Pan W and Shi S-L 2006 Electrical conductivity and dielectric properties of multiwalled carbon nanotube and alumina composites *Appl. Phys. Lett.* **89** 133122–3

[5] Yu A, Itkis M E, Bekyarova E and Haddon R C 2006 Effect of single-walled carbon nanotube purity on the thermal conductivity of carbon nanotube-based composites *Appl. Phys. Lett.* **89** 133102–3

[6] Velasco-Santos C, Martinez-Hernandez A L, Fisher F T, Ruoff R and Castano V M 2003 Improvement of thermal and mechanical properties of carbon nanotube composites through chemical functionalization *Chem. Mater.* **15** 4470–75

[7] Gong X, Liu J, Baskaran S, Voise R D and Young J S 2000 Surfactant-assisted processing of carbon nanotube/polymer composites *Chem. Mater.* **12** 1049–52

[8] Islam M F, Rojas E, Bergey D M, Johnson A T and Yodh A G 2003 High weight fraction surfactant solubilization of single-wall carbon nanotubes in water *Nano Lett.* **3** 269–73

[9] Wong E W, Sheehan P E and Lieber C M 1997 Nanobeam mechanics: elasticity, strength and toughness of nanorods and nanotubes *Science* **277** 1971–5

[10] Mahanandia P, Schneider J J, Khaneft M, Stühn B, Peixoto T P and Drossel B 2010 Polymer confinement effects in aligned carbon nanotubes arrays *Phys. Chem. Chem. Phys.* **12** 4407

[11] Hong K M and Noolandi J 1981 Theory of inhomogeneous multicomponent polymer systems *Macromolecules* **14** 727–36

[12] Helfand E 1975 Theory of inhomogeneous polymers: fundamentals of the Gaussian random-walk model *J. Chem. Phys.* **62** 999–1005

[13] Matsen M W and Schick M 1994 Stable and unstable phases of a diblock copolymer melt *Phys. Rev. Lett.* **72** 2660

[14] Mueller M and Schmid F 2005 Incorporating fluctuations and dynamics in self-consistent field theories for polymer blends *Advanced Computer Simulation Approaches for Soft Matter Sciences II* (*Advances in Polymer Science* vol 185/2005) ed C Holm and K Kremer (Berlin: Springer) pp 1–58

[15] Ceniceros H D and Fredrickson G H 2004 Numerical solution of polymer self-consistent field theory *Multiscale Model. Simul.* **2** 452–74

[16] Rasmussen K Ø and Kalosakas G 2002 Improved numerical algorithm for exploring block copolymer mesophases *J. Polym. Sci.* **40** 1777–83

[17] Carmesin I and Kremer K 1988 The bond fluctuation method: a new effective algorithm for the dynamics of polymers in all spatial dimensions *Macromolecules* **21** 2819–23

[18] Carmesin I and Kremer K 1990 Static and dynamic properties of two-dimensional polymer melts *J. Physique* **51** 18

[19] Wittmann H-P and Kremer K 1990 Vectorized version of the bond fluctuation method for lattice polymers *Comput. Phys. Commun.* **61** 309–30

[20] Paul W, Binder K, Heermann D W and Kremer K 1991 Crossover scaling in semidilute polymer solutions: a Monte Carlo test *J. Physique* **1** 24

[21] Paul W, Binder K, Heermann D W and Kremer K 1991 Dynamics of polymer solutions and melts. Reptation predictions and scaling of relaxation times *J. Chem. Phys.* **95** 7726–40

[22] Shaffer J S 1994 Effects of chain topology on polymer dynamics: bulk melts *J. Chem. Phys.* **101** 4205

[23] Müller M 2005 The bond fluctuation model and other lattice models *Handbook of Materials Modeling* part B ed S Yip (Dordrecht: Springer) pp 2599–606

[24] Metropolis N, Rosenbluth A W, Rosenbluth M N, Teller A H and Teller E 1953 Equation of state calculations by fast computing machines *J. Chem. Phys.* **21** 1087

[25] Hastings W K Monte Carlo sampling methods using Markov chainstheir applications 1970 *Biometrika* **57** 97–109

[26] Gerroff I, Milchev A, Binder K and Paul W 1993 A new off-lattice Monte Carlo model for polymers: a comparison of static and dynamic properties with the bond-fluctuation model and application to random media *J. Chem. Phys.* **98** 6526